European Journal of Medicinal Chemistry 277 (2024) 116767

Contents lists available at ScienceDirect

European Journal of Medicinal Chemistry

journal homepage: www.elsevier.com/locate/ejmech

Research paper

In vitro and in vivo evaluation of Bombesin-MMAE conjugates for targeted tumour therapy

Jacopo Gomena [a,b,c], Daniela Modena [d], Paola Cordella [d], Balázs Vári [e,f], Ivan Ranđelović [e,g], Adina Borbély [h], Michela Bottani [d], Diána Vári-Mező [b,c,e,f], Gábor Halmos [i], Éva Juhász [j], Christian Steinkühler [d], József Tóvári [e], Gábor Mező [b,c,*]

[a] Hevesy György PhD School of Chemistry, Eötvös Loránd University, 1117, Budapest, Hungary
[b] Eötvös Loránd University, Faculty of Science, Institute of Chemistry, 1117, Budapest, Hungary
[c] HUN-REN-ELTE Research Group of Peptide Chemistry, 1117, Budapest, Hungary
[d] Italfarmaco S.p.A., Preclinical R&D Department, 20092, Cinisello Balsamo (Milan), Italy
[e] Department of Experimental Pharmacology and the National Tumor Biology Laboratory, National Institute of Oncology, 1122, Budapest, Hungary
[f] School of Ph.D. Studies, Doctoral School of Pathological Sciences, Semmelweis University, 1085, Budapest, Hungary
[g] KINETO Lab Ltd., 1037, Budapest, Hungary
[h] MTA-ELTE Lendület Ion Mobility Mass Spectrometry Research Group, 1117, Budapest, Hungary
[i] Department of Biopharmacy, Faculty of Pharmacy, University of Debrecen, 4032, Debrecen, Hungary
[j] Department of Pediatrics, Faculty of Medicine, University of Debrecen, 4032, Debrecen, Hungary

ARTICLE INFO

Keywords:
Targeted tumour therapy
Bombesin
Peptide-drug conjugates
Thiol-maleimide conjugation
Cleavable linkers
Prostate cancer
Breast cancer

ABSTRACT

Targeted tumour therapy has proved to be an efficient alternative to overcome the limitations of conventional chemotherapy. The upregulation of the bombesin receptor 2 (BB2) in several malignancies and the advantages offered by peptide drug conjugates over antibody drug conjugates in terms of production and tumour targeting motivated us to synthesise and test bombesin conjugates armed with the tubulin binder monomethyl auristatin E. The widely used Val-Cit-PABC was initially included as cathepsin cleavable self-immolative linker for the release of the free drug. However, the poor stability of the Val-Cit-conjugates in mouse plasma encouraged us to consider the optimised alternatives Glu-Val-Cit-PABC and Glu-Gly-Cit-PABC. Conjugate **BN-EVcM1**, featuring Glu-Val-Cit-PABC, combined suitable stability ($t_{(½)}$ in mouse and human plasma: 8.4 h and 4.6 h, respectively), antiproliferative activity *in vitro* (IC_{50} = 29.6 nM on the human prostate cancer cell line PC-3) and the full release of the free payload within 24 h. Three conjugates, namely **BN-EGcM1**, **BN-EVcM1** and **BN-EVcM2**, improved the accumulation of MMAE in PC-3 human prostate cancer xenograft mice models, compared to the administration of the free drug. Among them, **BN-EVcM1** also stood out for the significantly extended survival of mice in *in vivo* acute efficacy studies and for the significant inhibition of the growth of a PC-3 tumour in mice in both acute and chronic efficacy studies.

1. Introduction

From the beginning of the 21st century, targeted cancer therapy has emerged as a valid alternative to conventional chemotherapy. The first FDA approval in year 2000 of the antibody drug conjugate (ADC) gemtuzumab ozogamicin (Mylotarg®) by Wyeth/Pfizer encouraged an increasing number of biopharmaceutical industries and research groups to invest in this technology. Currently, 13 ADCs are approved by FDA and/or EMA in oncology, six for treating haematological malignancies and seven against solid tumours. About 70 are in clinical development [1]. However, despite the primary goal of improving the safety of chemotherapeutics, ADCs are not devoid of side effects, most of which are off-target, off-tumour toxicities [2]. Furthermore, they exhibit unfavourable properties such as poor tumour penetration and immunogenicity. The manufacturing costs are high and antibodies with unspecific conjugation sites afford batches containing a mixture of ADCs with heterogenic drug-to-antibody ratios (DAR). The conjugation of a cytotoxic payload to peptides to obtain peptide drug conjugates (PDCs) is a promising way to overcome these drawbacks: their synthesis and manufacture are generally straightforward, cheap and afford conjugates

* Corresponding author. Eötvös Loránd University, Faculty of Science, Institute of Chemistry, 1117, Budapest, Hungary.
E-mail address: gabor.mezo@ttk.elte.hu (G. Mező).

https://doi.org/10.1016/j.ejmech.2024.116767
Received 3 July 2024; Received in revised form 6 August 2024; Accepted 11 August 2024
Available online 13 August 2024

with well-defined stoichiometries, preserved affinities for the target and improved accumulation at the tumour site [3]. Unfortunately, PDCs still have to find their way into the market. So far, only three products are approved for treatment: ^{177}Lu vipivotide tetraxetan (Pluvicto®) for castration-resistant prostate cancer, melphalan flufenamide (Melflufen®) for multiple myeloma and ^{177}Lu-DOTATATE (Lutathera®) for gastroenteropancreatic neuroendocrine tumour [4–6]. Nevertheless, many others are currently undergoing clinical trials, such as BT8009, BT5528, BT1718 by Bicycle Therapeutics [7–11], PEN-221 by Tarveda Therapeutics [12–14], ^{64}Cu SAR-Bombesin by Clarity Pharmaceutical [15] and several more exploiting ^{177}Lu for theragnostic purposes [16–21]. Although the majority of the mentioned PDCs are radiopharmaceuticals, radioligand therapy (RLT) still raises serious concerns for patients: because of the released radioactivity, the administration must take place in special controlled areas by healthcare professionals who are qualified and authorised to handle radiopharmaceutical products. Patients must avoid close contact with family members, children and pregnant women and sleep in separated rooms for several days after treatment. On the other hand, less stringent precautions would suffice for operating with conjugates that do not carry radioactive payloads. For this reason, we decided to focus on PDCs that exert their activity through cytotoxic payloads, such as daunomycin and monomethyl auristatin E (MMAE). The former is an anthracycline that intercalates DNA and subsequently inhibits topoisomerase II, whereas the latter is a potent microtubule targeting agent (MTA) and is the payload of the marketed ADCs Adcetris® (brentuximab vedotin – Seagen/Takeda), Polivy® (polatuzumab vedotin – Genentech), Padcev® (enfortumab vedotin – Astellas/Seagen) and Tivdak® (tisotumab vedotin – Seagen) and of both BT5528 and BT8009. In all of them, MMAE is conjugated to the targeting agent through the Val-Cit-PABC cathepsin B labile self-immolative spacer.

The BB2 receptor, a GPCR part of the bombesin receptors family, is overexpressed in prostate, breast, ovarian and small cell lung cancers, among others [22–26], and has gained attention throughout the years as a putative target for selective tumour therapy. Previous studies involving bombesin derivatives as targeting ligands have mainly focused on the production of radioconjugates as diagnostics or theragnostics, a handful reaching clinical trials [15,18,27–29]. However, the advantageous conjugation of potent cytotoxic agents to bombesin was barely considered. We have previously attached several bombesin derivatives to daunomycin to identify the most suitable homing peptide for targeted therapy of prostate and breast cancer models overexpressing the BB2 receptor, both *in vitro* and *in vivo* [26]. Two compounds, namely **L5** and **L6**, inhibited the tumour growth by about 30 % compared to the control group and significantly reduced the doubling time in mice xenografted with a human prostate cancer PC-3 cell line. To note, **L6** featured a novel homing bombesin derivative developed by our group.

In this work, we describe the *in vitro* and *in vivo* antiproliferative activity, stability and payload release kinetics of novel bombesin-based conjugates armed with MMAE. A first set of bioconjugates including the widely used Val-Cit-PABC spacer was produced after evaluating the affinities of **L5**-and **L6**-related peptides. These structures were further optimised by incorporating a PEG_4 module and the novel spacers Glu-Val-Cit-PABC or Glu-Gly-Cit-PABC to obtain more potent compounds with enhanced pharmacokinetic properties (Fig. 1). The second generation of PDCs complied with the expectations, demonstrating suitable stability in human and mouse plasma, improved distribution of the cytotoxic payload in the tumour in mice bearing a subcutaneously inoculated PC-3 human prostate tumour and significant prolonged survival and tumour growth inhibition in similar mice models.

2. Results

2.1. Binding affinity and selection of bombesin derivatives

Based on the homing peptide sequences that we had previously identified as suitable for tumour targeting [26], we assessed the affinity of seven bombesin analogues with or without Cys at the *C*-/N-terminus, to be later exploited for conjugation to MMAE. The results of the radioligand competitive binding assay on the three bombesin receptors are reported in Table 1. Our main interest was to find affine and selective analogues for the BB2 receptor. It is evident that the presence of Nle and

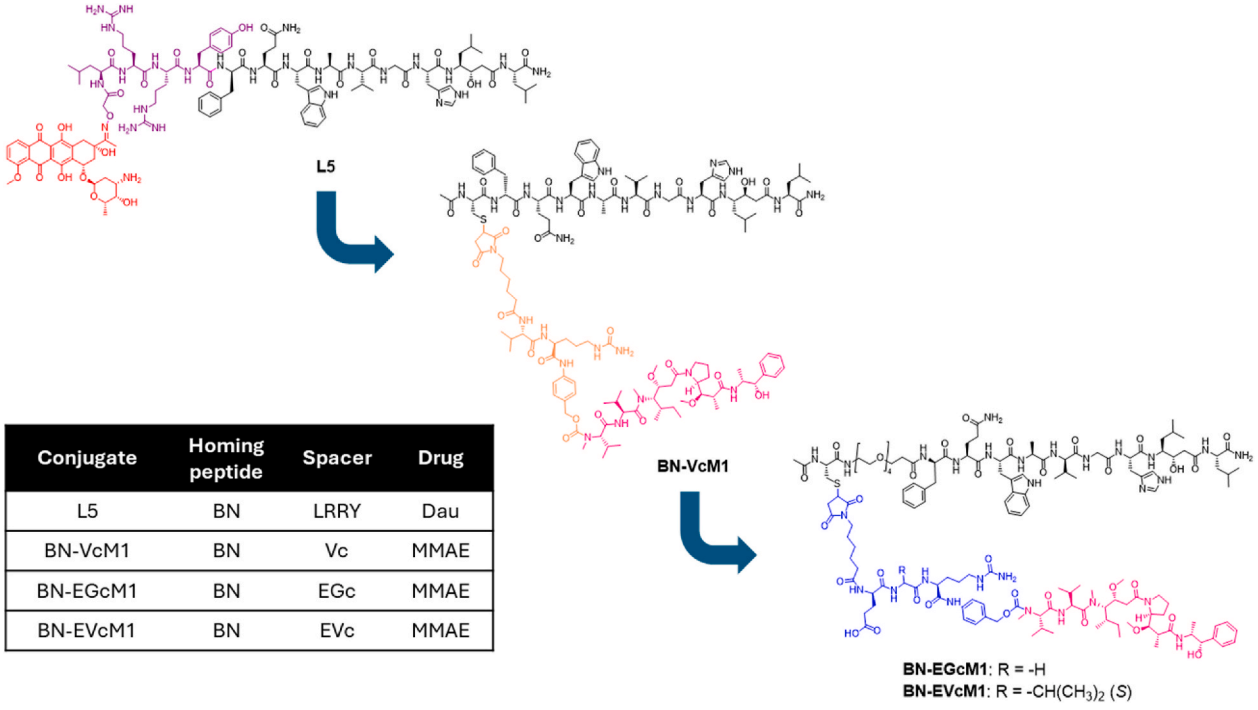

Conjugate	Homing peptide	Spacer	Drug
L5	BN	LRRY	Dau
BN-VcM1	BN	Vc	MMAE
BN-EGcM1	BN	EGc	MMAE
BN-EVcM1	BN	EVc	MMAE

Fig. 1. Evolving generations of bombesin conjugates. The observations on tumour growth inhibition and stability led to the optimised structures of **BN-EGcM1** and **BN-EVcM1**. Daunomycin is depicted in red, MMAE in pink. The spacers (Aoa)-Leu-Arg-Arg-Tyr, maleimidocaproyl Val-Cit-PABC and maleimidocaproyl Glu-Gly/Val-Cit-PABC in purple, orange and blue, respectively.

Table 1
Sequences and binding affinities of novel bombesin analogues towards the three bombesin receptors BB1, BB2 and BB3.

Peptide	Sequence	Affinity IC_{50} (nM)		
		BB1	BB2	BB3
ITA01	Ac-D-Phe-Gln-Trp-Ala-Val-Gly-His-Sta-Nle-Cys-NH_2	>10000	>10000	>10000
ITA02	Ac-D-Phe-Gln-Trp-Ala-Val-β-Ala-His-Sta-Nle-Cys-NH_2	>10000	>10000	>1000
ITA03	Ac-D-Phe-Gln-Trp-Ala-Val-Sar-His-Sta-Nle-Cys-NH_2	>10000	>10000	>1000
ITA04	Ac-D-Phe-Gln-Trp-Ala-Val-Gly-His-Sta-Leu-Cys-NH_2	>10000	>10000	10.1
ITA08	Ac-Cys-D-Phe-Gln-Trp-Ala-Val-Gly-His-Sta-Leu-NH_2	>10000	20.5	>1000
FP3	Ac-D-Phe-Gln-Trp-Ala-Val-Gly-His-Sta-Leu-NH_2	>10000	3.14	1.11
FP4	Ac-D-Phe-Gln-Trp-Ala-Val-β-Ala-His-Sta-Nle-NH_2	>10000	>10000	>10000

Cys at the C-terminus (**ITA01**–**04** and **FP4**) significantly hampered the affinity towards all the receptors, whereas the Sta–Leu bond seems crucial for the binding to BB2. Notably, the addition of the N-terminal Cys improved the selectivity towards this receptor: compared to **FP3**, the IC_{50} of **ITA08** for BB2 only diminished by about six times, whereas the binding to BB3 is nearly lost. As a result, we generated a first set of PDCs based on **ITA08** and the widely used VcMMAE linker-drug system (**BN-VcM1** – **BN-VcM1S**).

2.2. Synthesis and characterisation of the first generation BN-conjugates

2.2.1. Design, synthesis and binding affinity

Conjugate **BN-VcM1** was obtained *via* a thiol Michael addition between the N-terminal Cys of **ITA08** and the maleimide of VcMMAE (Fig. 2). **BN-VcM2** and **BN-VcM3** only differ in the substitution of Gly^{11} to either β-Ala or Sar, reported to improve the selectivity for BB2 [30] and reinforce the Gly^{11}–His^{12} bond [31,32], respectively. Two more PDCs were produced: one based on **FP4** (**BN-VcM4**), and another based on a scrambled version of **ITA08** (**BN-VcM1S**). While **BN-VcM1** and **BN-VcM3** maintained the selectivity towards BB2, with IC_{50} values in the low nanomolar range (41.8 nM and 36.3 nM, respectively), the affinity for any receptor dropped in the case of **BN-VcM2** (Table 2). **BN-VcM4**, containing an identical substitution, reported the same unsatisfactory binding. Therefore, we proved that β-Ala is not an appropriate replacement to Gly^{11} in analogues including the C-terminal Sta–Leu/Sta–Nle dipeptide. On the other hand, as expected, the scrambled **BN-VcM1S** lost both the affinity and selectivity that characterise the parent peptide **ITA08** and **BN-VcM1**.

Table 2
BN-VcMMAE conjugates affinities towards bombesin receptors and sequences of their homing peptides.

Conjugate	Peptide Sequence	Affinity IC_{50} (nM)		
		BB1	BB2	BB3
BBN-VcM1	Ac-Cys-D-Phe-Gln-Trp-Ala-Val-Gly-His-Sta-Leu-NH_2	>10000	41.8	5533
BBN-VcM2	Ac-Cys-D-Phe-Gln-Trp-Ala-Val-β-Ala-His-Sta-Leu-NH_2	>10000	5288	5250
BBN-VcM3	Ac-Cys-D-Phe-Gln-Trp-Ala-Val-Sar-His-Sta-Leu-NH_2	>10000	36.3	3598
BBN-VcM4	Ac-Cys-D-Phe-Gln-Trp-Ala-Val-β-Ala-His-Sta-Nle-NH_2	>10000	2181	>10000
BBN-VcM1S	Ac-Cys-Val-Sta-D-Phe-Gln-Gly-Leu-Ala-Trp-His-NH_2	>10000	4745	>10000

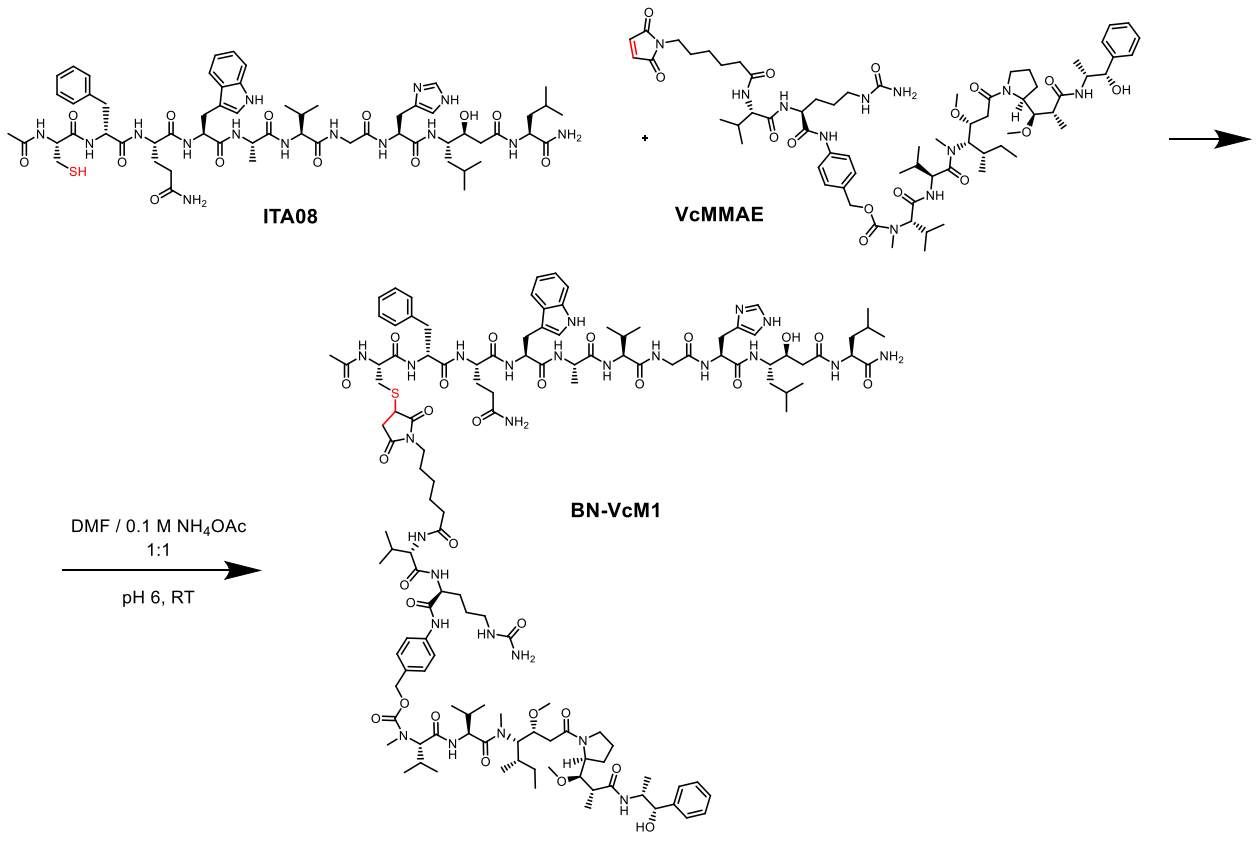

Fig. 2. Thiol Michael addition between the thiol of Cys^5 in **ITA08** and the maleimide in **VcMMAE** to generate conjugate **BN-VcM1**. The same reaction was used to obtain all the conjugates.

2.2.2. Cytotoxicity on PC-3 and MDA-MB-231

The antiproliferative activity of the VcMMAE conjugates was assessed on cell lines reported to overexpress the BB2 receptor: the human prostate cancer cell line PC-3 and the human breast cancer cell line MDA-MB-231. Surprisingly, despite the different affinities, all the five conjugates reported similar half-maximal inhibitory concentrations (IC_{50}) on both cell lines (Table 3). The greater efficacy on PC-3 correlates with the higher expression of BB2 compared to MDA-MB-231 [26]. Moreover, it is worth noticing that the extension of the incubation time for further 72 h reduces the IC_{50} by about seven times on PC-3 and five to six times on MDA-MB-231, independently from the renewal of the treatment. Given that the same trend was observed for the MMAE treatment, we deduced that it is due to the mechanism of action of the drug that affects actively proliferating cells and therefore leads to increased potency the more cell divisions are allowed to occur upon drug exposure.

The inactivity of the conjugates on cells that do not express bombesin receptors was demonstrated on the Chinese hamster ovary cells CHO–K1 (Table S3, Supplementary Materials).

2.2.3. Stability in human and mouse plasma

A crucial parameter to investigate when developing conjugates for targeted cancer therapy is their stability. Parenteral injection is the preferred route of administration, so, conjugates must remain intact in circulation until the tumour environment is reached. Conjugates **BN-VcM1** – **BN-VcM4** were thus incubated in both human and mouse plasma for 24 h at a concentration of 5 μM. No substantial differences were observed among the metabolic stabilities of the conjugates. Despite satisfactory half-lives ($t_{(½)}$) in human plasma, ranging from 8.2 h (**BN-VcM1**) to 12 h (**BN-VcM4**), all the four conjugates were impressively labile in mouse plasma, releasing the free MMAE within minutes ($t_{(½)}$ ~7–8 min), therefore, hampering a further preclinical assessment of their activity *in vivo* (Fig. S21, Supplementary Materials). To our knowledge such a poor stability of the Val-Cit linker has never been recorded in similar conjugates [8,33,34]. We attributed the premature hydrolysis of the linker to the action of the extracellular carboxylesterase 1c (Ces1c) [35,36].

This event, together with the apparent lack of affinity-dependent cytotoxicity of the conjugates, encouraged us to optimise their structure. To this aim, we included a polyethylene glycol (PEG_4) moiety before the N-terminal Cys of the peptides and switched to spacers based on the Glu-Val-Cit (EVc) and Glu-Gly-Cit (EGc) tripeptides. On the one hand, Jamous et al. advised on the optimal length of the PEG_4 linker to obtain bombesin derivatives with improved pharmacokinetic properties [37]. On the other hand, EVc and EGc spacers are reported to have superior stabilities in the bloodstream thanks to their resistance to Ces1c and human neutrophil elastase mediated degradation [36,38]. As peptide carriers, we used the N-terminal pegylated versions of **ITA08** and [Nle^{14}]BBN(6–14), supposedly an agonist of BB2 [30,39–41]. For both, variants carrying a Trp^8/Bta^8 substitution, reported to improve the biodistribution of bombesin derivatives while minimising the accumulation in the pancreas [42], were also synthesised (Fig. 3). All the new peptides were conjugated to MMAE *via* Cys thiol-maleimide Michael addition.

Table 3
Half-maximal inhibitory concentrations obtained by treating PC-3 and MDA-MB-231 cells with VcMMAE-conjugates and free MMAE for 72 h or 72 + 72 h. Values are reported as mean ± SD, n = 3. In the case of **BN-VcM1S**, n = 1.

Compound	72 h		72 + 72 h (single treatment)		72 + 72 h (double treatment)	
	PC-3 (IC_{50}, nM)	MDA-MB-231 (IC_{50}, nM)	PC-3 (IC_{50}, nM)	MDA-MB-231 (IC_{50}, nM)	PC-3 (IC_{50}, nM)	MDA-MB-231 (IC_{50}, nM)
BN-VcM1	717.6 ± 60.9	888.2 ± 76.7	101.0 ± 8.6	202.4 ± 20.0	92.1 ± 7.4	154.9 ± 37.6
BN-VcM2	850.0 ± 13.8	1127.9 ± 94.5	161.8 ± 4.5	235.5 ± 12.3	152.5 ± 8.5	220.8 ± 10.2
BN-VcM3	938.5 ± 37.2	1279.3 ± 139.4	167.6 ± 2.3	268.2 ± 36.1	142.8 ± 4.3	228.4 ± 9.6
BN-VcM4	851.9 ± 277.1	1282.1 ± 287.1	131.5 ± 7.9	218.4 ± 39.3	120.6 ± 17.0	175.9 ± 12.0
BN-VcM1S	828.0	642.7	182.6	163.0	296.6	173.7
MMAE	3.4 ± 0.7	37.3 ± 22.2	0.9 ± 0.2	0.5 ± 0.1	0.7 ± 0.1	0.3 ± 0.1

2.3. Synthesis and characterisation of second generation BN-conjugates

2.3.1. Synthesis of BBN-EGcMMAE and BBN-EVcMMAE conjugates

The synthesis of both EGcMMAE and EVcMMAE spacer-drug modules started by the solid phase peptide synthesis (SPPS) of maleimidocaproyl-Glu(OtBu)-AA-Cit-OH on a 2-chlorotrityl resin (Fig. 4). The protected peptides were cleaved off the resin and elongated at their C-terminal free carboxylic acid by coupling to the amino functional group of *p*-aminobenzyl alcohol, using EEDQ as coupling agent, for 24 h under argon atmosphere. The primary alcohol was then activated as *p*-nitrophenyl carbonate by a 3 h reaction with bis *p*-nitrophenyl carbonate under nitrogen. The reaction between the secondary amine of MMAE and the carbonate afforded a carbamate bond between the drug and the spacer. Finally, the *t*-butyl protection of the glutamic acid was removed in TFA/H_2O/TIS (95:2.5:2.5 v/v/v%) and a Michael addition between the thiol of the N-terminal Cys of each bombesin analogues and the maleimide on the spacer-drug module was performed. Purification *via* RP-HPLC afforded ≥98 % pure compounds.

2.3.2. Binding affinity of second-generation BN-conjugates

The affinity of the optimised set of conjugates for BB2 was measured using a radioligand displacement assay on PC-3 and MDA-MB-231 cell lines, naturally expressing the receptor. The results are reported in Table 4. Furthermore, the measurements were repeated on the first-generation conjugates, revealing consistent results with the first experiment, performed on CHO–K1 cells (Table S4, Supplementary Materials). Similarly to this group, the optimised conjugates showed affinities in the low nanomolar range, on both cell lines (Table 4). By and large, the IC_{50} values were lower for PDCs featuring a Sta^{13}–Leu^{14}-based bombesin analogue (the lowest on both PC-3 and MDA-MB-231 by **BN-EVcM1**: 59.4 ± 8.88 nM and 69.5 ± 10.3 nM, respectively) compared to the more conventional sequences based on [Nle^{14}]BBN(6–14) (the highest on PC-3 by **BN-EVcM3**: 101.2 ± 9.8 nM, on MDA-MB-231 by **BN-EVcM4**: 106.1 ± 10.3 nM). Moreover, compounds were slightly more affine for PC-3 cells than MDA-MB-231, in line with the reported higher expression of BB2 by the former cell line [26]. We deduced that the insertion of the PEG_4 module and the modification of the linker and the peptide sequence did not affect the binding to BB2. As a result, we expected retained biological activities.

2.3.3. Plasma stability of second generation BN-conjugates

Conjugates **BN-EGcM1** and **BN-EVcM1** were used as models to evaluate whether the optimised spacers could improve the mouse plasma stability of the VcMMAE-based compounds (**BN-VcM1** – **BN-VcM4**). Therefore, the new conjugates were tested using the same conditions as the first set: compounds were incubated in human and mouse plasma at 37 °C at a concentration of 5 μM and aliquots were collected at the beginning of the assay (t_0) and after 0.25, 0.5, 1, 2, 4 and 24 h. The LC-HRMS analysis revealed preserved stability in human plasma, significantly improved half-lives in mouse plasma, and a negligible loss of free payload too. A direct comparison of conjugates **BN-VcM1**, **BN-EGcM1** and **BN-EVcM1**, differing only in the spacer and the presence or absence of PEG_4, confirmed the successful optimisation strategy (Fig. 5A and B, Table 5; Table S5 and Fig. S21, Supplementary

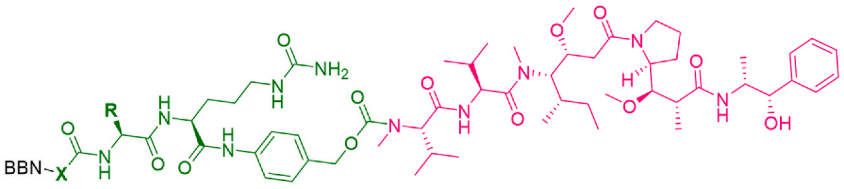

	Conjugate	BBN analogue	Spacer		
			X	R	Di- or Tripeptide
First Generation	**BN-VcM1**	Cys-D-Phe-Gln-Trp-Ala-Val-Gly-His-Sta-Leu-NH_2	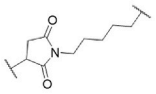	-$CH(CH_3)_2$	Val-Cit
	BN-VcM2	Cys-D-Phe-Gln-Trp-Ala-Val-βAla-His-Sta-Leu-NH_2			
	BN-VcM3	Cys-D-Phe-Gln-Trp-Ala-Val-Sar-His-Sta-Leu-NH_2			
	BN-VcM4	Cys-D-Phe-Gln-Trp-Ala-Val-βAla-His-Sta-Nle-NH_2			
Second Generation	**BN-EGcM1**	Cys-PEG4-D-Phe-Gln-Trp-Ala-Val-Gly-His-Sta-Leu-NH_2	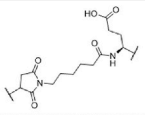	H	Glu-Gly-Cit
	BN-EGcM2	Cys-PEG4-D-Phe-Gln-Bta-Ala-Val-Gly-His-Sta-Leu-NH_2			
	BN-EGcM3	Cys-PEG4-Asn-Gln-Trp-Ala-Val-Gly-His-Leu-Nle-NH_2			
	BN-EGcM4	Cys-PEG4-Asn-Gln-Bta-Ala-Val-Gly-His-Leu-Nle-NH_2			
	BN-EVcM1	Cys-PEG4-D-Phe-Gln-Trp-Ala-Val-Gly-His-Sta-Leu-NH_2	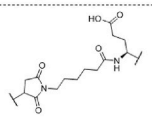	-$CH(CH_3)_2$	Glu-Val-Cit
	BN-EVcM2	Cys-PEG4-D-Phe-Gln-Bta-Ala-Val-Gly-His-Sta-Leu-NH_2			
	BN-EVcM3	Cys-PEG4-Asn-Gln-Trp-Ala-Val-Gly-His-Leu-Nle-NH_2			
	BN-EVcM4	Cys-PEG4-Asn-Gln-Bta-Ala-Val-Gly-His-Leu-Nle-NH_2			

Fig. 3. The two new sets of MMAE-conjugates. The self-immolative spacer is depicted in green, MMAE in pink. Amino acid substitutions in the sequence of the bombesin analogues are highlighted in different colours. Bta: benzothienyl alanine; Sar: sarcosine, *N*-methyl glycine; Sta: statine.

Materials, for all the half-lives and MMAE release).

The stability in human and mouse plasma of all the remaining optimised conjugates was later tested too. The half-lives of conjugates carrying a bombesin derivative based on [Nle^{14}]BBN(6–14) were shortened to about 2–3 h, as opposed to those with an analogue based on **ITA08**, which generally showed $t_{(½)} \geq 5$ h, and consistency among conjugates with the same spacer (Table S5 and Fig. S21, Supplementary Materials).

2.3.4. *Cytotoxicity of second generation BN-conjugates*

The cytotoxicity of the new set of eight conjugates was assessed on the PC-3, MDA-MB-231 and CHO–K1 wt cell lines. All in all, the antiproliferative activity on PC-3 and MDA-MB-231 was spacer-dependent: the four EGcMMAE-conjugates showed decreased activity compared to the four EVcMMAE-conjugates (Table 6). None of the conjugates resulted active on the BB2 negative cell line CHO–K1 wt (Table S3, Supplementary Materials). Surprisingly, while conjugates with the EGc linker were only slightly more active than the first set of VcMMAE-conjugates, the conjugates that included the EVc linker displayed about more than thirty times higher activities on PC-3 cells. Especially, conjugates **BN-EVcM1** and **BN-EVcM2** showed IC_{50} values as low as 29.6 ± 2.3 nM and 29.3 ± 2.9 nM for an incubation of 72 h, and 3.5 ± 0.9 nM and 4.0 ± 1.3 nM when the treatment was extended for 72 more hours. This difference reflects the greater ability to release the free payload by EVcMMAE conjugates compared to the EGcMMAE set, as shown below. Moreover, we ensured that the observed cytotoxicity was not caused by a premature release of the MMAE from the conjugates before entering the cellular compartment by testing the stability of many conjugates in DMEM containing 10 % FBS over 72 h. Although the detected fraction of conjugates decreased over time, the only metabolite that we identified was the intact conjugate with a partially hydrolysed thiosuccinimide, whereas no free MMAE was detected (Table S5 and Fig. S21, Supplementary Materials). Since not only this well-known ring opening reaction is a cause of minor changes, but is also reported to stabilise the structure of the PDCs [43–45], we concluded that it would not affect their antiproliferative efficacy.

Given the big gap of antiproliferative activity between conjugates carrying the same homing peptide but a different spacer, we were interested in delving into the causes of this event. Therefore, we investigated the efficiency of the release of MMAE in a lysosomal homogenate.

2.3.5. *MMAE release in lysosomal homogenate by VcMMAE-, EGcMMAE- and EVcMMAE-Conjugates*

The cleavage of the self-immolative cathepsin-labile spacers, which allows the release of the free MMAE in the lysosomes, was assessed by incubating conjugates **BN-VcM1**, **BN-EGcM1** and **BN-EVcM1** in rat liver lysosomal homogenate at 37 °C, sampling at t_0 and after 0.25, 0.5, 1, 2, 4, and 24 h (Fig. 5C). MMAE was quantified by LC-HRMS with the aid of an internal standard. A nearly full release of the payload was witnessed in the case of the well-established maleimidocaproyl Val-Cit-PABC spacer already after half an hour, and maleimidocaproyl Glu-Val-Cit-PABC, after 24 h. To note, the latter released *ca*. 90 % of the drug after 4 h. On the other hand, only 4 % of the drug could be detected after 24 h incubation of the EGc-linker based **BN-EGcM1** in lysosomes. While this proved the higher IC_{50} values of this class of conjugates compared to those that include EVcMMAE, we were surprised to witness a considerable difference in the release of the drug between two conjugates with comparable *in vitro* antiproliferative activity (**BN-VcM1** and **BN-EGcM1**). We hypothesize that other factors, like the absence of the PEG linker in the set of VcMMAE-conjugates, confer unique physicochemical properties, thus influencing solubility, internalisation, and intracellular pathway of the conjugate.

2.3.6. *Ex vivo biodistribution of **BN-EGcM1**, **BN-EVcM1**, **BN-EVcM2**, **BN-EVcM4** and free MMAE*

Considering the results discussed so far, we aimed to compare how conjugates with different homing peptides and spacers performed *in vivo*. Therefore, the biodistribution of conjugates **BN-EGcM1** and **BN-EVcM1** was tested to directly compare the linker chemistry, whereas **BN-EVcM2** and **BN-EVcM4** were included for a comparison in terms of targeting capabilities. Only one EGcMMAE-conjugate took part in the experiment because of the demonstrated superior antiproliferative activity and MMAE release efficiency of EVcMMAE-conjugates. Despite the poorer plasma stability compared to the other three conjugates, **BN-EVcM4** was involved to evaluate any difference in tumour targeting

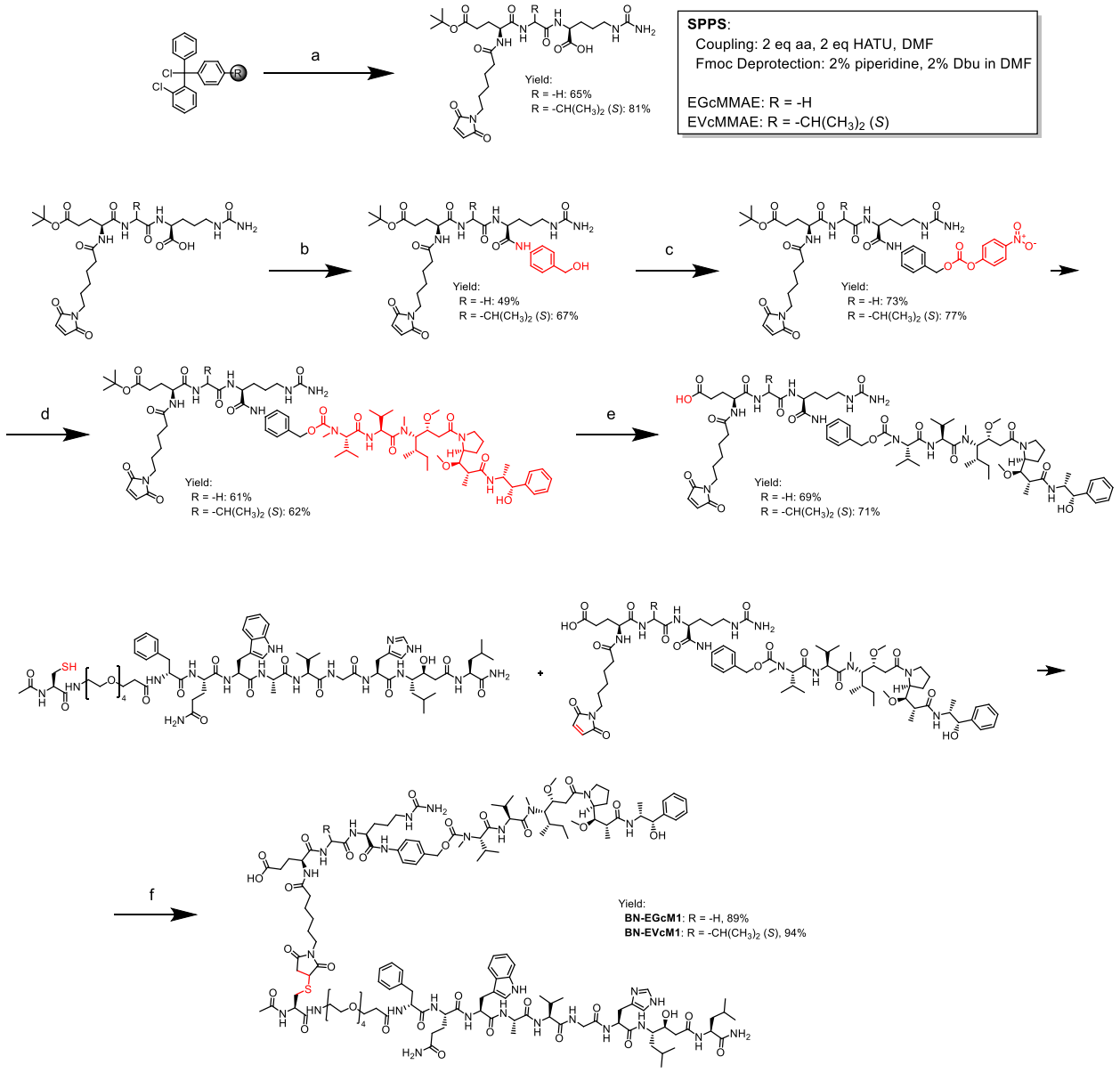

Fig. 4. (**A**) Synthesis of EGcMMAE and EVcMMAE and (**B**) conjugation to the homing peptide to generate either compound **BN-EGcM1** or **BN-EVcM1**. Conditions: a) (I) SPPS, (II) acetic acid/TFE/DCM 1:1:3 v/v/v, 90 min, RT; b) *p*-aminobenzyl alcohol, EEDQ in DCM/MeOH 2:1 v/v, N_2 atm., 24 h, RT; c) bis(4-nitrophenyl) carbonate, DIPEA in dry DMF, N_2 atm., 3 h, RT; d) MMAE, HOBt, DIPEA in DMF, o/n, RT; e) TFA/TIS/H_2O 95:2.5:2.5 v/v/v%, 10 min, RT; f) 0.1 M NH_4OAc/DMF 1:1, pH 6, RT (immediate).

between agonists, such as the peptide carrier of **BN-EVcM4**, and antagonists of BB2 (all the others). The biodistribution of the mentioned PDCs was compared to that of free MMAE in PC-3 bearing mice. Compounds were injected intraperitoneally (i.p.) and the levels of MMAE were measured in blood, heart, kidney, liver, lungs, pancreas, and tumour after 1, 6 and 24 h and quantified as percentage of injected dose per gram of tissue (%ID/g) (Fig. 6). The four conjugates were all able to deliver a higher amount of drug to the tumour environment than the free MMAE, up to 7.8 times at the 6 h time point in the case of **BN-EVcM1** (Fig. 6F and G). On the other hand, no drug could be detected in any tissue 24 h after the administration of **BN-EVcM4**, probably because of the poorer circulation half-life (Fig. 6D). As a matter of fact, the blood concentration of the conjugate was already very low at the 1 h time point (0.35 % ID/g), suggesting a fast clearance (Table S6, Supplementary Materials). The highest levels of released MMAE were found after 1 h in the liver and the kidneys for all the conjugates, in line with the expected metabolism and excretion route. However, they decreased substantially 6 h and 24 h post injection (Fig. 6A–D and Table S6). Notably, MMAE was cleared from every organ except for the kidneys, the liver, and the tumour site 24 h after the treatment with **BN-EGcM1**, **BN-EVcM1** and **BN-EVcM2**, indicating the preferential accumulation of the conjugates in the malignant tissue (Fig. 6A–C). One of the major limitations of bombesin derivatives is the considerable distribution to the pancreas, especially at early time points, due to the high expression of the BB2 receptor and the cross-reactivity between the human and murine homologues [31,46–49]. Nevertheless, among our four conjugates, only **BN-EVcM4** accumulated extensively in the pancreas (%ID/g at 6 h: 10.1 % intact conjugate and 3.55 % released MMAE, Table S6), likely as a consequence of its agonist nature. This undesired event, together with the fast excretion of **BN-EVcM4**, strengthens the claim that BB2 antagonists might be better than agonists for tumour targeting, motivated us to discard this conjugate and continue the *in vivo* investigation with **BN-EGcM1**, **BN-EVcM1** and **BN-EVcM2**.

Table 4
Affinity of the optimised conjugates on the BB2-expressing human cancer cell lines PC-3 (prostate) and MDA-MB-231 (breast). Values are reported as mean ± SD, n = 3.

Compound	Sequence	Affinity IC_{50} (nM)	
		PC-3	MDA-MB-231
BN-EGcM1	Cys-PEG_4-D-Phe-Gln-Trp-Ala-Val-Gly-His-Sta-Leu-NH_2	68.3 ± 2.56	72.9 ± 0.31
BN-EGcM2	Cys-PEG_4-D-Phe-Gln-Bta-Ala-Val-Gly-His-Sta-Leu-NH_2	71.1 ± 5.38	76.9 ± 2.88
BN-EGcM3	Cys-PEG_4-Asn-Gln-Trp-Ala-Val-Gly-His-Leu-Nle-NH_2	83.2 ± 13.4	79.3 ± 9.18
BN-EGcM4	Cys-PEG_4-Asn-Gln-Bta-Ala-Val-Gly-His-Leu-Nle-NH_2	80.7 ± 8.34	82.4 ± 7.11
BN-EVcM1	Cys-PEG_4-D-Phe-Gln-Trp-Ala-Val-Gly-His-Sta-Leu-NH_2	59.4 ± 8.88	69.5 ± 10.3
BN-EVcM2	Cys-PEG_4-D-Phe-Gln-Bta-Ala-Val-Gly-His-Sta-Leu-NH_2	58.2 ± 1.59	70.4 ± 9.94
BN-EVcM3	Cys-PEG_4-Asn-Gln-Trp-Ala-Val-Gly-His-Leu-Nle-NH_2	101.2 ± 9.8	97.4 ± 5.55
BN-EVcM4	Cys-PEG_4-Asn-Gln-Bta-Ala-Val-Gly-His-Leu-Nle-NH_2	93.6 ± 7.12	106.1 ± 10.3

2.3.7. *In vivo acute efficacy study*

The tumour growth inhibition of **BN-EGcM1**, **BN-EVcM1** and **BN-EVcM2** was firstly assessed on mice bearing a subcutaneously inoculated PC-3 human prostate tumour by a single i.p. administration of 2 mg/kg conjugates (MMAE-content) and compared to free MMAE (1 mg/kg). In all the treated groups, except that of **BN-EGcM1** and the control, the animal body weight decreased in the days following the treatment. The toxicity was regarded as moderate because the average body weight loss did not reach the critical 20 % reduction (Fig. 7A) and the general condition of mice based on behavioural indicators (activity, state of coat and stool, paleness etc.) did not change significantly. However, the body weight recovered over time.

Very early, on day 14 after cell inoculation (day 5 after treatment), three animals treated with free MMAE had already lost 20 % of their body weight, and they had to be sacrificed (Fig. 7B). Even if the free MMAE was administered at halved doses than the drug content of PDCs, it caused consistent toxicity, that led to the sacrifice of the last animal of this group on day 38 after cell inoculation, resulting in a median survival of 24.5 days (Table 7). This median survival was lower than that of the control group (33 days), which animals were sacrificed mostly due to reaching the pre-defined cut-off tumour volume of 2000 mm^3. On the other hand, the three groups of mice treated with the PDCs showed significantly prolonged survival, both compared to the control and to the MMAE groups. The median survival of mice treated with **BN-EVcM1** was exactly 2-fold higher than that of mice treated with MMAE (49 vs. 24.5 days). Moreover, the **BN-EVcM1** group revealed significantly higher survival compared to mice treated with **BN-EVcM2**, suggesting a superior therapeutic index.

Free MMAE also gave the worst tumour volume inhibition. It was significantly different than the control only on day 14, while in the following days the tumour volume was even higher than the control (Fig. 7C). The **BN-EVcM2** group, which had the worse survival among the PDCs, revealed an unsatisfactory antitumor activity too, with a significant effect only on day 21. The tumour volume of mice in the **BN-EGcM1** group was significantly reduced compared to the control group from day 14 to day 28, whereas the antitumor effect of **BN-EVcM1** was significant in comparison to the control throughout the whole

Table 5
Direct comparison of the half-lives in mouse and human plasma of conjugates **BN-VcM1**, **BN-EGcM1** and **BN-EVcM1**, having the same targeting peptide and payload, differing in the spacer. McVc-PABC: maleimidocarpoyl-Val-Cit-*p*-aminobenzoyl carbamate; McEGc-PABC: maleimidocarpoyl-Glu-Gly-Cit-*p*-aminobenzoyl carbamate; McEVc-PABC: maleimidocarpoyl-Glu-Val-Cit-*p*-aminobenzoyl carbamate.

Conjugate	Spacer	Stability	
		Human plasma (t ½, h)	Mouse plasma (t ½, h)
BN-VcM1	McVc-PABC	8.2	0.12
BN-EGcM1	McEGc-PABC	5.1	7.2
BN-EVcM1	McEVc-PABC	4.6	8.4

Table 6
Half-maximal inhibitory concentrations of the optimised conjugates and MMAE on PC-3 and MDA-MB-231 cell lines (72 h or 72 + 72 h incubation). Values are reported as mean ± SD, n = 2 or 3.

Compound	72 h		72 + 72 h (single treatment)		72 + 72 h (double treatment)	
	PC-3 (IC_{50}, nM)	MDA-MB-231 (IC_{50}, nM)	PC-3 (IC_{50}, nM)	MDA-MB-231 (IC_{50}, nM)	PC-3 (IC_{50}, nM)	MDA-MB-231 (IC_{50}, nM)
BN-EGcM1	428.3 ± 71.4	884.7 ± 2.4	110.3 ± 6.6	163.6 ± 12.1	83.5 ± 2.4	131.4 ± 17.1
BN-EGcM2	586.3 ± 23.0	943.3 ± 105.7	142.5 ± 5.0	170.8 ± 15.1	116.5 ± 3.9	130.4 ± 22.5
BN-EGcM3	830.4 ± 19.9	1260.0 ± 73.0	248.5 ± 1.2	270.1 ± 24.2	200.0 ± 10.2	216.7 ± 9.0
BN-EGcM4	782.2 ± 149.8	1255.5 ± 322.5	215.5 ± 1.3	267.5 ± 51.9	165.4 ± 7.7	217.2 ± 36.8
BN-EVcM1	29.6 ± 1.8	525.6 ± 119.3	4.8 ± 0.5	42.3 ± 0.1	3.5 ± 0.9	43.3 ± 0.1
BN-EVcM2	29.3 ± 2.4	298.9 ± 23.0	6.0 ± 0.5	41.0 ± 0.5	4.0 ± 1.3	39.9 ± 0.8
BN-EVcM3	64.1 ± 0.8	343.8 ± 7.5	18.2 ± 2.2	60.1 ± 6.0	12.6 ± 0.3	52.7 ± 6.7
BN-EVcM4	53.9 ± 1.9	500.6 ± 61.3	15.6 ± 1.3	48.7 ± 6.5	11.8 ± 0.5	46.4 ± 2.7
MMAE	7.21 ± 1.0	10.1 ± 5.0	0.4 ± 0.2	0.2 ± 0.01	0.3 ± 0.1	0.2 ± 0.04

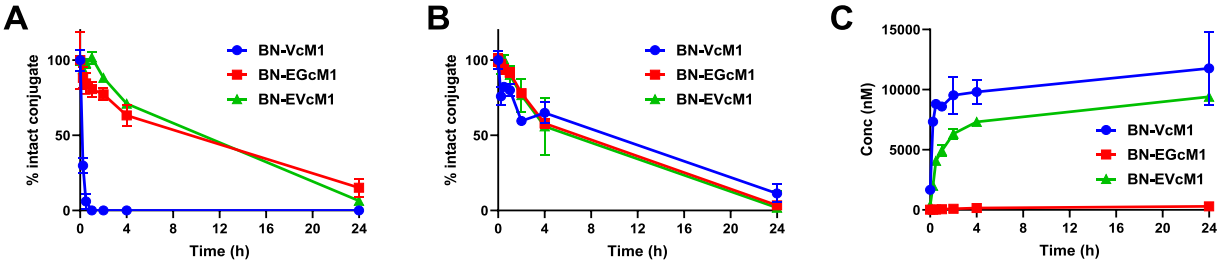

Fig. 5. Stability of conjugates **BN-VcM1, BN-EGcM1** and **BN-EVcM1** in mouse (**A**) and human plasma (**B**), respectively. (**C**) MMAE released from conjugates upon incubation in lysosomal homogenate. Data points are reported as mean ± SD, n = 2.

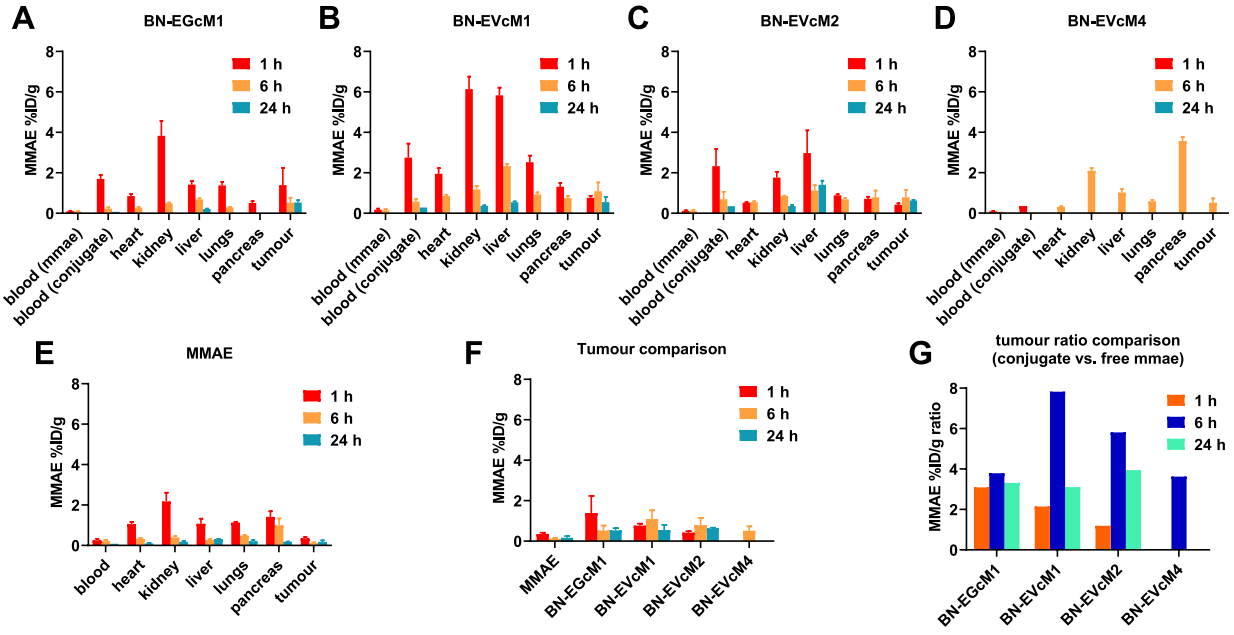

Fig. 6. (**A**–**E**) Biodistribution of the conjugates and free MMAE expressed as %ID/g ± SD of detected MMAE in each district (n = 3). (**F**) Direct comparison of MMAE accumulation at the tumour site upon administration of either the conjugates or free MMAE. (**G**) Ratio between MMAE detected at the tumour site upon administration of each conjugate and free MMAE.

experiment.

On day 38, when the last animals in the control and MMAE groups were sacrificed, the tumour volume was reduced by 15.9 %, 26.3 %, 34.2 %, and 65.2 % by MMAE, **BN-EGcM1**, **BN-EVcM2** and **BN-EVcM1**, respectively.

2.3.8. In vivo chronic efficacy

In a follow-up experiment we investigated the chronic efficacy of the compounds by four treatments at reduced doses of both the conjugates (0.5 mg/kg MMAE-content) and the free MMAE (0.2 mg/kg). Mouse weight gradually decreased in all groups, but no severe weight loss occurred. However, free MMAE-treated mice showed the highest bodyweight decrease upon treatment. These reductions regularly recovered in a couple of days after the treatment.

The chronic treatment results were in line with the acute study, showing the superior efficacy of **BN-EVcM1** over the other conjugates (Fig. 8A). **BN-EVcM2** exhibited the lowest toxicity, but poorer efficacy too (Fig. 8B). Interestingly, the chronic treatment with **BN-EGcM1** caused skin rash as severe adverse event. Because of this and the quick weight loss upon **BN-EGcM1** treatment, mice treated with this conjugate were terminated earlier than the rest of the groups.

BN-EVcM1 and **BN-EVcM2** were both able to significantly inhibit tumour growth compared to both controls and free MMAE. This effectivity was observed both by tumour weight (Fig. 8C) and tumour size (Fig. 8D) at the end of the experiment. **BN-EVcM1** reduced the tumour weight by 41.6 % and the tumour size by 59.8 %. **BN-EVcM2** reduced the tumour weight by 26 % and the tumour size by 48 %. Finally, when comparing the normalized liver weights, no significant change was detected compared to controls in any of the treatment groups (data not shown).

3. Conclusion

Motivated by the discovery of two promising bombesin-based Dau-conjugates for the treatment of prostate cancer [26], we decided to generate new PDCs carrying the potent tubulin inhibitor monomethyl auristatin E (MMAE) to improve the efficacy. The unspecific antiproliferative activity on the human cancer cell lines PC-3 and MDA-MB-231 and the impressive lability in murine plasma of this first set of compounds demanded structure optimisation. Therefore, the second generation of MMAE-conjugates included the reinforced Glu-Gly-Cit-PABC or Glu-Val-Cit-PABC self-immolative spacers and a PEG_4 module. The modifications provided more stable compounds to be tested *in vivo* on murine models. Moreover, **BN-EVcM1** – **BN-EVcM4** displayed enhanced cytotoxicity on both PC-3 and MDA-MB-231 cell lines, with an IC_{50} as low as 29.6 ± 1.8 nM on PC-3 in the case of **BN-EVcM1**, supported by the full release of MMAE within 24 h in a lysosomal homogenate. The biodistribution of **BN-EGcM1**, **BN-EVcM1** and **BN-EVcM2** on PC-3 bearing mice showed an improved accumulation of the payload at the tumour site 1, 6 and 24 h post-injection compared to the free MMAE. This was reflected by the enhanced tumour growth inhibition by the three conjugates compared to both the control and free MMAE in both the acute and chronic antitumor efficacy studies. **BN-EVcM1** significantly inhibited the PC-3 tumour growth compared to the control, by 65.2 % and 59.8 % in tumour size, respectively. **BN-EVcM2** also gave a significant reduction of the tumour size in the chronic study, by 48 % compared to the control. Moreover, MMAE revealed far greater toxicity than the PDCs, both after single and repeated administrations.

In conclusion, we report the design and optimisation of PDCs based on bombesin analogues as targeting devices and armed with MMAE as cytotoxic payload. We ascertained the superiority of Glu-Gly-Cit and Glu-Val-Cit as compared to Val-Cit spacers for the *in vivo* investigation of antitumor conjugates, which we included in the conjugates to treat prostate cancer. Two of them, namely **BN-EVcM1** and **BN-EVcM2**, significantly inhibited the growth of a s.c. inoculated PC-3 human prostate cancer in mice and successfully improved the safety of free MMAE, significantly extending the survival of mice. Therefore, we highlight their outstanding targeting ability and efficacy in the treatment of tumours overexpressing BB2 receptor. Although our conjugates demonstrated satisfactory accumulation at the tumour site, sufficient to provide significant antiproliferative effects, the biodistribution of

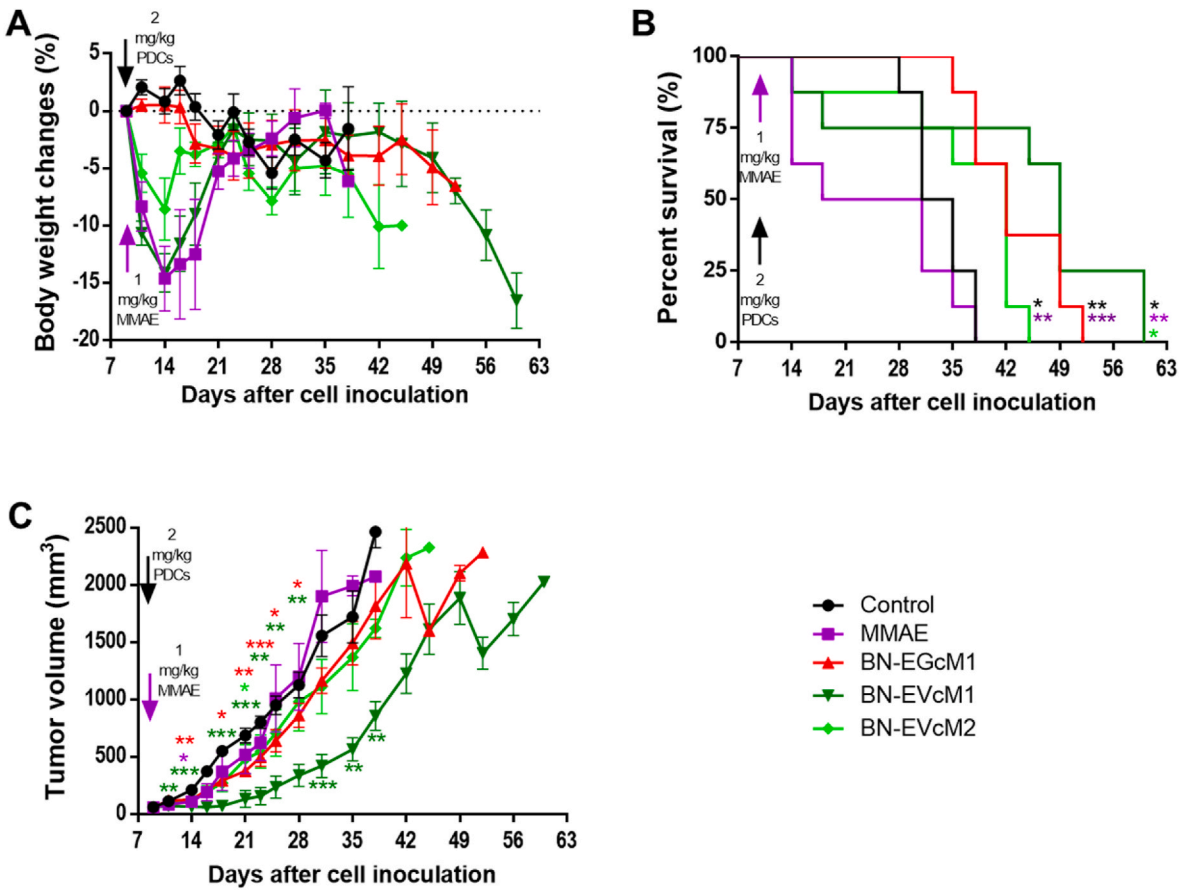

Fig. 7. Effect of MMAE-conjugates (2 mg/kg MMAE content, black arrow) and free MMAE (1 mg/kg, red arrow) on subcutaneous PC-3 human prostate cancer xenograft model in acute *in vivo* efficacy study. (**A**) Animal body weight change (% to the start of treatment, average ± SEM). (**B**) Animal survival in percentage. (**C**) Tumour volume (mm^3, average ± SEM), eight animals per group. Statistical analysis for the survival data performed using Log-rank (Mantel-Cox) test, while Mann–Whitney test was applied for the tumour growth inhibition. *, ** and *** represent significance at $p \leq 0.05$, $p \leq 0.01$ and $p \leq 0.001$, respectively. Dotted line in body weight graph (A) represents the body weight when treatment was applied (zero changes). * Black, purple and light green in survival graph (B) indicate significant difference compared to the control, free MMAE and **BN-EVcM2** groups respectively. * Purple, red, dark green and light green in tumour volume graph (C) indicate significant difference of free MMAE, **BN-EGcM1**, **BN-EVcM1** and **BN-EVcM2** groups compared to the control.

Table 7
Survival of animals bearing subcutaneous PC-3 human prostate cancer under single treatment with MMAE-conjugates (2 mg/kg, MMAE content) and free MMAE (1 mg/kg).

Group	Median survival (days)	Log-rank (Mantel-Cox) test (p-value)		
		vs Control	vs MMAE	vs BN-EVcM2
Control	33	–	–	–
MMAE	24.5	0.1858	–	–
BN-EGcM1	42	0.0021	0.0005	–
BN-EVcM1	49	0.0167	0.0047	0.0209
BN-EVcM2	42	0.03	0.0077	–

bombesin-based conjugates still remains a notable weakness. Strategies focused on the improvement of tumour accumulation may be key to achieve clinically relevant activities.

4. Experimental section

4.1. Synthesis of the conjugates – conjugation of the peptides to spacer-MMAE via thio-michael addition

Intermediates Mc-Glu-Gly-Cit-PABC-MMAE, Mc-Glu-Val-Cit-PABC-MMAE, or the commercially available VcMMAE (1 eq) and each bombesin analogue (1.2 eq) were dissolved in a 1:1 mixture of DMF and NH_4OAc buffer (pH 6), RT. Every reaction immediately reached completeness and was directly purified *via* RP-HPLC. Column: Daisogel ODS-RPS C18 column (250 × 10 mm, 10 μm). Eluents: H_2O + 0.1 % TFA (A) and H_2O/MeCN 20:80 v/v% + 0.1 % TFA (B). Method: 30–85 % eluent B gradient in 50 min, flow rate: 6 mL/min. The desired fractions were lyophilised to afford conjugates as soft white solids with ≥95 % purity:

Detailed synthesis procedures of the peptides and spacer-MMAE modules, RP-HPLC chromatograms and ESI-HRMS spectra of the tested peptides and conjugates are reported in the Supplementary Materials.

4.2. Biological and biochemical evaluation

4.2.1. Receptor binding affinity

Binding characteristics of bombesin receptors and conjugates on membrane preparations from PC-3 and MDA-MB-231 cancer cells were determined by ligand competition assays using ^{125}I-labeled [Tyr^4]-bombesin (Code No: NEX258, Revvity Inc., Waltham, MA, USA), as reported previously [50,51]. Binding of bombesin conjugates to cancer cell membranes was measured in displacement experiments based on competitive inhibition of ^{125}I-[Tyr^4]-bombesin binding using various concentrations of peptide conjugates (10 μM–10 pM). IC_{50} was defined as the concentration of bombesin conjugate causing 50 % inhibition of ^{125}I-[Tyr^4]-bombesin binding.

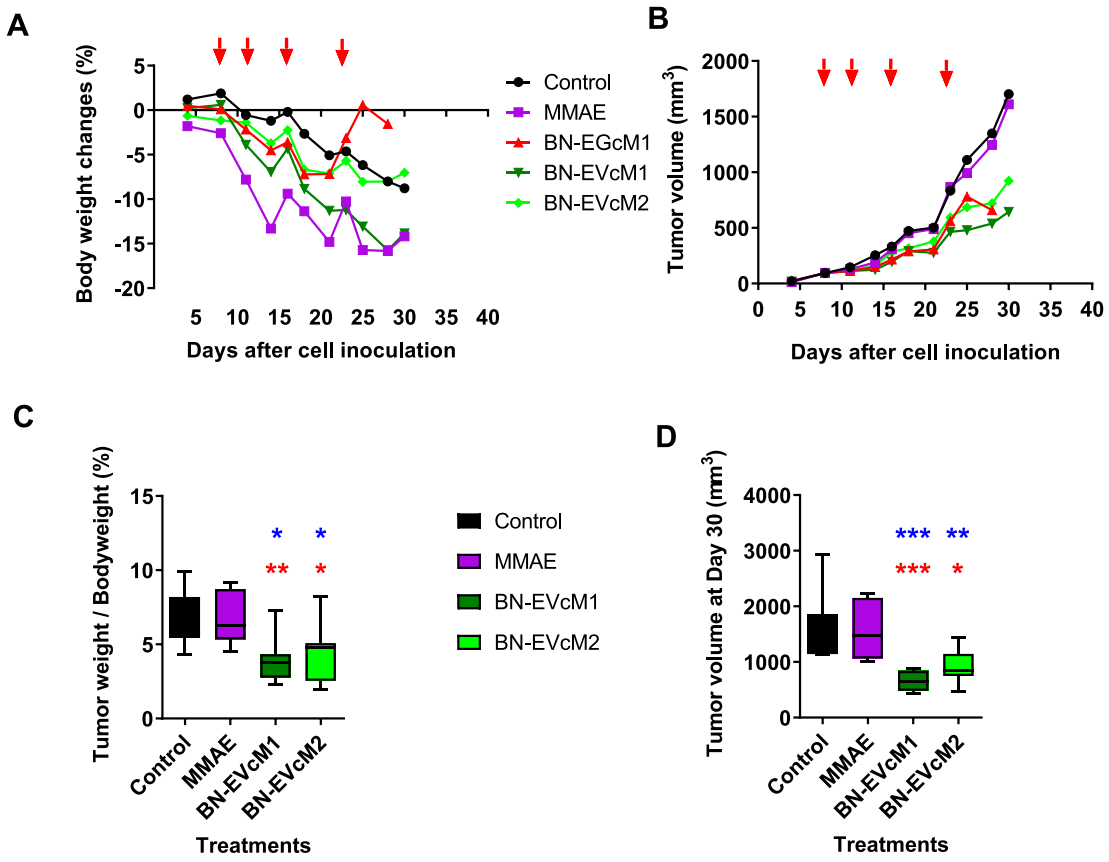

Fig. 8. Chronic effect of PDCs and free MMAE on tumour growth. (**A**) Change in bodyweight of mice during the experiment. The red arrows indicate treatment days. (**B**) Change of tumour size over the experiment. The red arrows indicate treatment days. (**C**) Tumour weight over bodyweight ratios at the end of the experiment. **BN-EVcM1** and **BN-EVcM2** showed significant inhibition of tumour growth (p-value vs. control = 0.0175 and 0.0396, respectively; p-value vs. MMAE group = 0.0070 and 0.0379, respectively). (**D**) Tumour sizes at the end of the experiment. **BN-EVcM1** and **BN-EVcM2** showed significant inhibition of tumour growth (p-value vs. control = 0.0006 and 0.0070, respectively; p-value vs. MMAE group = 0.0006 and 0.0111, respectively). Significant differences compared to the control or MMAE group are depicted with blue or red *, respectively.

4.2.2. *In vitro cytotoxicity*

Handling information for the cell lines used in the assay are reported in the Supplementary Materials.

The day following the incubation, cells were treated with serial dilutions of each compound, starting at 2000 nM for the conjugates and 100 nM for MMAE, and incubated for 72 h. Then, either the experiment was terminated, or the incubation continued for further 72 h after in one case replacing the supernatant with fresh medium or, in the other case, repeating the treatment. In each case, at least two independent experiments were performed, with three replicates per concentration. Wells treated with 0.05 % DMSO served as control. Cell-free wells containing medium served as blanks. At the end of the treatments, 100 μL of medium were replaced with 20 μL CellTiter 96® Aqueous (Promega, Italy) and the plates incubated for 90 min (37 °C, 5 % CO_2). The absorbance at λ = 490 nm was measured using a Victor^2 1420 Multilabel Counter (PerkinElmer) and the cell viability was calculated as the absorbance corrected by the background signal, divided by the corrected absorbance of untreated control wells. The half-maximal inhibitor concentrations (IC_{50}) were extrapolated by fitting the data using non-linear regression through Prism (GraphPad Software).

4.2.3. *Stability of the conjugates in human and mouse plasma and cell culture medium*

Stability of the conjugates in mouse and human plasma and DMEM +10 % FBS was evaluated after incubation of the samples at 37 °C and a concentration of 5 μM up to 24 h (plasma) or 1 μM up to 72 h (cell culture medium), in duplicates. At established sampling points (t_0, 0.25, 0.5, 1, 2, 4 and 24 h) aliquots of each sample were quenched with 1 % formic acid in MeCN (2 × volume excess), to stop the reaction precipitating plasma proteins or large FBS components. Samples were then centrifuged for 10 min, at 14000 rpm, 4 °C, and the supernatants diluted 1:1 with dH_2O prior analysis. Samples were analysed using a LC-HRMS system constituted by a Vanquish Flex connected to an Orbitrap QExactive Focus (Thermo Scientific). Chromatographic separation was conducted using an Aeris peptide column (3.6 μm, XB-C18, 50 × 2.1 mm) (Phenomenex), at 40 °C, with a flow rate of 0.4 mL/min and a gradient composed of 90 % water/10 % acetonitrile, 0.1 % formic acid (eluent A) and 0.1 % formic acid in acetonitrile (eluent B). Analyses were performed using a HESI source in positive full scan mode (*m/z* range: 450–3000). Management of sample analysis was carried out using Chromeleon 7.2.8 (Thermo Scientific).

4.2.4. *MMAE release in rat liver lysosomal homogenate*

The payload release was assessed according to a previously published protocol [26]. Details are reported in the Supplementary Materials.

4.3. *In vivo experiments*

General Laboratory Practice are reported in the Supplementary Materials.

4.3.1. *Biodistribution in PC-3 bearing mice*

The biodistribution of **BN-EGcM1**, **BN-EVcM1**, **BN-EGcM2**, and **BN-EVcM4** was compared to that of free MMAE. A single treatment was administered intraperitoneally (i.p.) in a dose of 2 mg/kg per mice.

Animals were split into three groups, and samples were obtained 1 h, 6 h and 24 h after treatment. Samples included blood, tumour, and organs such as liver, kidneys, heart, lungs, and pancreas. Detailed procedures regarding sample collection from animals are reported in the Supplementary Materials.

Frozen organs and primary tumours were pooled based on treatment groups. Tissue samples were weighed accurately, collected and homogenised in sterile distilled water (1:2 w/v) using gentleMACS™ Dissociator (Miltenyi Biotec, Bergisch Gladbach, Germany). Homogenates were centrifuged for 5 min at 600 g, 4 °C, and 200 μL aliquots of supernatant were stored at −20 °C o/n into LoBind® tubes. The leftovers were frozen for further analysis. The following day they were thawed at RT and diluted in 40 μL of 5 % w/v $ZnSO_4$ (ThermoFisher Scientific, Waltham, Massachusetts, USA) and 600 μL of MeCN/MeOH 90:10 v/v% containing [Tyr^4]BBN as internal standard, for protein precipitation. The tubes were vortexed vigorously and stored at −20 °C o/n. The frozen blood samples were thawed at RT and treated likewise. The samples were then centrifuged for 30 min, 10000 g, 4 °C and the supernatant diluted with an equal volume of dH_2O + 0.1 % formic acid. The tubes were centrifuged again for 15 min, 10000 g, 4 °C and the supernatants analysed by LC-HRMS to detect the levels of MMAE using an UltiMate 3000 UHPLC system coupled to a Q ExactiveTM Focus, high-resolution and high-mass accuracy, hybrid quadrupole-orbitrap mass spectrometer.

4.3.2. *In vivo acute efficacy study*

Conjugates **BN-EGcM1**, **BN-EVcM1**, **BN-EGcM2** and free MMAE were involved in both acute and chronic *in vivo* efficacy studies.

A single treatment was administered by i.p. injection in a volume of 0.1 mL per animal, nine days after cells inoculation, when the average tumour volume was 62 mm^3. The mice were randomized and assigned to five groups consisting of eight animals for each treatment. The compounds were dissolved in 5 % DMSO (Sigma-Aldrich, St. Louis, MO, USA) in water for injection (Pharmamagist Kft., Budapest, Hungary). The PDCs dose was 2 mg/kg MMAE-content, while free MMAE was injected in a dose of 1 mg/kg of body weight. The mice in the control group were treated with the solvent.

Animal body weight and tumour volumes were measured initially when the treatment started and at periodic intervals. A digital calliper was used to measure the longest (a) and the shortest (b) diameter of a given tumour. The tumour volume was calculated using formula $V = ab^2 \times \pi/6$. The antitumor activity and the survival of animals were monitored by humane end-off points, and the animals were sacrificed by cervical dislocation when a 20 % body weight loss and/or a tumour volume of 2000 mm^3 were reached.

4.3.3. *In vivo chronic efficacy study*

Treatments were administered i.p. with an injection volume of 0.1 mL per animal, eight days after the cells were inoculated, when the average tumour volume was 93 mm^3. The mice were randomized and assigned to five groups consisting of seven animals for each treatment. The treatments were dissolved in 5 % DMSO (Sigma-Aldrich) in water for injection (Pharmamagist Kft.). The PDCs dose was 0.5 mg/kg MMAE-content, while free MMAE was injected in a dose of 0.2 mg/kg of body weight. The mice in the control group were treated with the solvent. Four treatments were administered at days 8, 11, 16 and 23.

Animal body weight and tumour volumes were measured initially when the treatment started and at periodic intervals. A digital calliper was used to measure the longest (a) and the shortest diameter (b) of a given tumour. The tumour volume was calculated using formula $V = ab^2 \times \pi/6$. Antitumor activity was monitored.

Funding

This research was funded by the European Union's Horizon 2020 research and innovation programme under the Marie Sklodowska-Curie Grant agreement No. 861316 (MagicBullet::Reloaded). This study was also supported by the National Research, Development and Innovation Fund of Hungary (NRDIF-OTKA K146039 to G.M.), the National Laboratories Excellence program, as part of the National Tumor Biology Laboratory project (2022-2.1.1-NL-2022-00010), and by the Hungarian Thematic Excellence Program (TKP2021-EGA-44). Further support was provided by the Thematic Excellence Programme TKP2021-EGA-20 (Biotechnology) (G.H.) that has been implemented with support provided by the Ministry of Culture and Innovation of Hungary from the National Research, Development and Innovation Fund, financed under the TKP2021-EGA funding scheme.

CRediT authorship contribution statement

Jacopo Gomena: Writing – review & editing, Writing – original draft, Visualization, Project administration, Methodology, Investigation, Formal analysis, Data curation, Conceptualization. **Daniela Modena:** Writing – review & editing, Writing – original draft, Supervision, Methodology, Investigation, Formal analysis, Conceptualization. **Paola Cordella:** Methodology, Formal analysis, Data curation. **Balázs Vári:** Writing – review & editing, Methodology, Investigation, Formal analysis. **Ivan Ranđelović:** Writing – review & editing, Methodology, Investigation, Formal analysis. **Adina Borbély:** Writing – review & editing, Methodology, Investigation, Formal analysis, Data curation. **Michela Bottani:** Methodology, Investigation, Formal analysis. **Diána Vári-Mező:** Methodology, Investigation, Formal analysis. **Gábor Halmos:** Writing – review & editing, Methodology, Investigation, Formal analysis. **Éva Juhász:** Methodology, Investigation, Formal analysis. **Christian Steinkühler:** Writing – review & editing, Supervision, Project administration, Funding acquisition. **József Tóvári:** Writing – review & editing, Project administration, Funding acquisition. **Gábor Mező:** Writing – review & editing, Supervision, Resources, Project administration, Methodology, Conceptualization, Funding acquisition.

Declaration of competing interest

Gabor Mezo reports financial support was provided by National Research, Development and Innovation Fund of Hungary. Gabor Halmos reports financial support was provided by National Research, Development and Innovation Fund of Hungary. Jozsef Tovari reports financial support was provided by National Research, Development and Innovation Fund of Hungary. Christian Steinkuhler reports financial support was provided by European Commission. Gabor Mezo reports financial support was provided by European Commission. If there are other authors, they declare that they have no known competing financial interests or personal relationships that could have appeared to influence the work reported in this paper.

Data availability

Data will be made available on request.

Appendix A. Supplementary data

Supplementary data to this article can be found online at https://doi.org/10.1016/j.ejmech.2024.116767.

References

[1] C. Dumontet, J.M. Reichert, P.D. Senter, J.M. Lambert, A. Beck, Antibody–drug conjugates come of age in oncology, Nat. Rev. Drug Discov. (2023), https://doi.org/10.1038/s41573-023-00709-2.
[2] P. Tarantino, B. Ricciuti, S.M. Pradhan, S.M. Tolaney, Optimizing the safety of antibody–drug conjugates for patients with solid tumours, Nat. Rev. Clin. Oncol. (2023), https://doi.org/10.1038/s41571-023-00783-w.
[3] B.M. Cooper, J. Iegre, D.H. O'Donovan, M. Ölwegård Halvarsson, D.R. Spring, Peptides as a platform for targeted therapeutics for cancer: peptide-drug conjugates

(PDCs), Chem. Soc. Rev. 50 (2021) 1480–1494, https://doi.org/10.1039/d0cs00556h.
[4] Pluvicto - Lutetium 177 Vipivotide Tetraxetan, 2022. https://www.ema.europa.eu/en/medicines/human/EPAR/pluvicto. (Accessed 20 September 2023).
[5] Pepaxti - Melphalan Flufenamide, 2023. https://www.ema.europa.eu/en/medicines/human/EPAR/pepaxti. (Accessed 20 September 2023).
[6] Lutathera - Lutetium 177 Oxodotreotide, 2018. https://www.ema.europa.eu/en/medicines/human/EPAR/lutathera. (Accessed 20 September 2023).
[7] M. Rigby, G. Bennett, L. Chen, G.E. Mudd, H. Harrison, P.J. Beswick, K. Van Rietschoten, S.M. Watcham, H.S. Scott, A.N. Brown, P.U. Park, C. Campbell, E. Haines, J. Lahdenranta, M.J. Skynner, P. Jeffrey, N. Keen, K. Lee, BT8009; A nectin-4 targeting bicycle toxin conjugate for treatment of solid tumors, Mol Cancer Ther 21 (2022) 1747–1756, https://doi.org/10.1158/1535-7163.MCT-21-0875.
[8] G.E. Mudd, H. Scott, L. Chen, K. Van Rietschoten, G. Ivanova-Berndt, K. Dzionek, A. Brown, S. Watcham, L. White, P.U. Park, P. Jeffrey, M. Rigby, P. Beswick, Discovery of BT8009: a nectin-4 targeting bicycle toxin conjugate for the treatment of cancer, J. Med. Chem. 65 (2022) 14337–14347, https://doi.org/10.1021/acs.jmedchem.2c00065.
[9] G. Bennett, A. Brown, G. Mudd, P. Huxley, K. van Rietschoten, S. Pavan, L. Chen, S. Watcham, J. Lahdenranta, N. Keen, MMAE delivery using the bicycle toxin conjugate BT5528, Mol Cancer Ther 19 (2020) 1385–1394, https://doi.org/10.1158/1535-7163.MCT-19-1092.
[10] C. Gowland, P. Berry, J. Errington, P. Jeffrey, G. Bennett, L. Godfrey, M. Pittman, A. Niewiarowski, S.N. Symeonides, G.J. Veal, Development of a LC-MS/MS method for the quantification of toxic payload DM1 cleaved from BT1718 in a Phase i study, Bioanalysis 13 (2021) 101–113, https://doi.org/10.4155/bio-2020-0256.
[11] U. Banerji, N. Cook, T.R.J. Evans, I. Moreno Candilejo, P. Roxburgh, C.L.S. Kelly, N. Sabaratnam, R. Passi, S. Leslie, S. Katugampola, L. Godfrey, N. Tremayne, G. Bennett, M. Koehler, G. Langford, S.N. Symeonides, M. Pittman, A Cancer Research UK phase I/IIa trial of BT1718 (a first in class Bicycle Drug Conjugate) given intravenously in patients with advanced solid tumours, J. Clin. Oncol. 36 (2018), https://doi.org/10.1200/JCO.2018.36.15_suppl.TPS2610. TPS2610–TPS2610.
[12] B.H. White, K. Whalen, K. Kriksciukaite, R. Alargova, T. Au Yeung, P. Bazinet, A. Brockman, M. Dupont, H. Oller, C.A. Lemelin, P. Lim Soo, B. Moreau, S. Perino, J.M. Quinn, G. Sharma, R. Shinde, B. Sweryda-Krawiec, R. Wooster, M.T. Bilodeau, Discovery of an SSTR2-targeting maytansinoid conjugate (PEN-221) with potent activity in vitro and in vivo, J. Med. Chem. 62 (2019) 2708–2719, https://doi.org/10.1021/acs.jmedchem.8b02036.
[13] K.A. Whalen, B.H. White, J.M. Quinn, K. Kriksciukaite, R. Alargova, T.P. Au Yeung, P. Bazinet, A. Brockman, M.M. DuPont, H. Oller, J. Gifford, C.A. Lemelin, P.L. Soo, S. Perino, B. Moreau, G. Sharma, R. Shinde, B. Sweryda-Krawiec, M.T. Bilodeau, R. Wooster, Targeting the somatostatin receptor 2 with the miniaturized drug conjugate, PEN-221: a potent and novel therapeutic for the treatment of small cell lung cancer, Mol Cancer Ther 18 (2019) 1926–1936, https://doi.org/10.1158/1535-7163.MCT-19-0022.
[14] D.M. Halperin, M.L. Johnson, J.A. Chan, L.L. Hart, N. Cook, V.M. Patel, B. L. Schlechter, J. Cave, A. Dowlati, L.S. Blaszkowsky, T. Meyer, J.R. Eads, D. Culp, K. Krikscіukaite, L. Mei, M. Bilodeau, J. Bloss, M.H. Kulke, The safety and efficacy of PEN-221 somatostatin analog (SSA)-DM1 conjugate in patients (PTS) with advanced GI mid-gut neuroendocrine tumor (NET): phase 2 results, J. Clin. Oncol. 39 (2021) 4110, https://doi.org/10.1200/JCO.2021.39.15_suppl.4110.
[15] K. Wong, G. Sheehan-Dare, A. Nguyen, B. Ho, V. Liu, J. Lee, L. Brown, R. Dear, L. Chan, S. Sharma, A. Malaroda, I. Smith, E. Lim, L. Emmett, 64Cu-SAR-Bombesin PET-CT imaging in the staging of estrogen/progesterone receptor positive, HER2 negative metastatic breast cancer patients: safety, dosimetry and feasibility in a phase I trial, Pharmaceuticals 15 (2022), https://doi.org/10.3390/ph15070772.
[16] V.P. Chavda, H.K. Solanki, M. Davidson, V. Apostolopoulos, J. Bojarska, Peptide-drug conjugates: a new Hope for cancer management, Molecules 27 (2022), https://doi.org/10.3390/molecules27217232.
[17] E. Heh, J. Allen, F. Ramirez, D. Lovasz, L. Fernandez, T. Hogg, H. Riva, N. Holland, J. Chacon, Peptide drug conjugates and their role in cancer therapy, Int. J. Mol. Sci. 24 (2023), https://doi.org/10.3390/ijms24010829.
[18] J. Kurth, B.J. Krause, S.M. Schwarzenböck, C. Bergner, O.W. Hakenberg, M. Heuschkel, First-in-human dosimetry of gastrin-releasing peptide receptor antagonist [177Lu]Lu-RM2: a radiopharmaceutical for the treatment of metastatic castration-resistant prostate cancer, Eur J Nucl Med Mol Imaging 47 (2020) 123–135, https://doi.org/10.1007/s00259-019-04504-3.
[19] J. McConathy, M. Dhawan, A. Goenka, E. Lim, Y. Menda, B. Chasen, M. Khushman, A. Mintz, Y. Zakharia, J. Sunderland, O. Bowles, J. Xiao, A. Simmons, K. Wride, A. Enke, T. Hope, Abstract CT251: LuMIERE: a phase 1/2 study investigating safety, pharmacokinetics, dosimetry, and preliminary antitumor activity of 177Lu-FAP-2286 in patients with advanced or metastatic solid tumors, Cancer Res. 82 (2022), https://doi.org/10.1158/1538-7445.AM2022-CT251. CT251–CT251.
[20] B.M. Privé, M.A. Boussihmad, B. Timmermans, W.A. van Gemert, S.M.B. Peters, Y. H.W. Derks, S.A.M. van Lith, N. Mehra, J. Nagarajah, S. Heskamp, H. Westdorp, Fibroblast activation protein-targeted radionuclide therapy: background, opportunities, and challenges of first (pre)clinical studies, Eur J Nucl Med Mol Imaging 50 (2023) 1906–1918, https://doi.org/10.1007/s00259-023-06144-0.
[21] R.P. Baum, C. Schuchardt, A. Singh, M. Chantadisai, F.C. Robiller, J. Zhang, D. Mueller, A. Eismant, F. Almaguel, D. Zboralski, F. Osterkamp, A. Hoehne, U. Reineke, C. Smerling, H.R. Kulkarni, Feasibility, biodistribution, and preliminary dosimetry in peptide-targeted radionuclide therapy of diverse adenocarcinomas using 177Lu-FAP-2286: first-in-humans results, J. Nucl. Med. 63 (2022) 415–423, https://doi.org/10.2967/jnumed.120.259192.
[22] S. Majumdar, T.J. Siahaan, Peptide-mediated targeted drug delivery, Med. Res. Rev. 32 (2012) 637–658, https://doi.org/10.1002/med.20225.
[23] J.C. Reubi, S. Wenger, J. Schmuckli-Maurer, J.-C. Schaer, M. Gugger, Bombesin receptor subtypes in human cancers: detection with the universal radioligand 125 I-[D-TYR 6 ,-ALA 11 , PHE 13 , NLE 14] bombesin(6-14). http://www.ncbi.nlm.nih.gov/, 2002.
[24] R.T. Jensen, J.F. Battey, E.R. Spindel, R.V. Benya, International union of pharmacology. LXVIII. Mammalian bombesin receptors: nomenclature, distribution, pharmacology, signaling, and functions in normal and disease states, Pharmacol. Rev. 60 (2008) 1–42, https://doi.org/10.1124/pr.107.07108.
[25] S.R. Preston, G. V Miller, J.N. Primrose, Bombesin-like Peptides and Cancer, 1996.
[26] J. Gomena, B. Vári, R. Oláh-Szabó, B. Biri-Kovács, S. Bősze, A. Borbély, Á. Soós, I. Ranđelović, J. Tóvári, G. Mező, Targeting the gastrin-releasing peptide receptor (GRP-R) in cancer therapy: development of bombesin-based peptide–drug conjugates, Int. J. Mol. Sci. 24 (2023), https://doi.org/10.3390/ijms24043400.
[27] L. Baratto, H. Duan, H. Mäcke, A. Iagaru, Imaging the distribution of gastrin-releasing peptide receptors in cancer, J. Nucl. Med. 61 (2020) 792–798, https://doi.org/10.2967/JNUMED.119.234971.
[28] B.A. Nock, P. Kanellopoulos, L. Joosten, R. Mansi, T. Maina, Peptide radioligands in cancer theranostics: agonists and antagonists, Pharmaceuticals 16 (2023), https://doi.org/10.3390/ph16050674.
[29] R. Mansi, B.A. Nock, S.U. Dalm, M.B. Busstra, W.M. van Weerden, T. Maina, Radiolabeled bombesin analogs, Cancers 13 (2021), https://doi.org/10.3390/cancers13225766.
[30] P. Hoppenz, S. Els-Heindl, A.G. Beck-Sickinger, Identification and stabilization of a highly selective gastrin-releasing peptide receptor agonist, J. Pept. Sci. 25 (2019), https://doi.org/10.1002/psc.3224.
[31] A. Accardo, F. Galli, R. Mansi, L. Del Pozzo, M. Aurilio, A. Morisco, P. Ringhieri, A. Signore, G. Morelli, L. Aloj, Pre-clinical evaluation of eight DOTA coupled gastrin-releasing peptide receptor (GRP-R) ligands for in vivo targeting of receptor-expressing tumors, EJNMMI Res. 6 (2016) 1–10, https://doi.org/10.1186/s13550-016-0175-x.
[32] A. Höhne, L. Mu, M. Honer, P.A. Schubiger, S.M. Ametamey, K. Graham, T. Stellfeld, S. Borkowski, D. Berndorff, U. Klar, U. Voigtmann, J.E. Cyr, M. Friebe, L. Dinkelborg, A. Srinivasan, Synthesis, 18F-labeling, and in vitro and in vivo studies of bombesin peptides modified with silicon-based building blocks, Bioconjug Chem 19 (2008) 1871–1879, https://doi.org/10.1021/bc800157h.
[33] S. Cazzamalli, A. Dal Corso, D. Neri, Linker stability influences the anti-tumor activity of acetazolamide-drug conjugates for the therapy of renal cell carcinoma, J. Contr. Release 246 (2017) 39–45, https://doi.org/10.1016/j.jconrel.2016.11.023.
[34] S. Boinapally, H.H. Ahn, B. Cheng, M. Brummet, H. Nam, K.L. Gabrielson, S. R. Banerjee, I. Minn, M.G. Pomper, A prostate-specific membrane antigen (PSMA)-targeted prodrug with a favorable in vivo toxicity profile, Sci. Rep. 11 (2021), https://doi.org/10.1038/s41598-021-86551-1.
[35] M. Dorywalska, R. Dushin, L. Moine, S.E. Farias, D. Zhou, T. Navaratnam, V. Lui, A. Hasa-Moreno, M.G. Casas, T.T. Tran, K. Delaria, S.H. Liu, D. Foletti, C. J. O'Donnell, J. Pons, D.L. Shelton, A. Rajpal, P. Strop, Molecular basis of valine-citrulline-PABC linker instability in site-specific ADCs and its mitigation by linker design, Mol Cancer Ther 15 (2016) 958–970, https://doi.org/10.1158/1535-7163.MCT-15-1004.
[36] Y. Anami, C.M. Yamazaki, W. Xiong, X. Gui, N. Zhang, Z. An, K. Tsuchikama, Glutamic acid-valine-citrulline linkers ensure stability and efficacy of antibody-drug conjugates in mice, Nat. Commun. 9 (2018), https://doi.org/10.1038/s41467-018-04982-3.
[37] M. Jamous, M.L. Tamma, E. Gourni, B. Waser, J.C. Reubi, H.R. Maecke, R. Mansi, PEG spacers of different length influence the biological profile of bombesin-based radiolabeled antagonists, Nucl. Med. Biol. 41 (2014) 464–470, https://doi.org/10.1016/j.nucmedbio.2014.03.014.
[38] S.Y.Y. Ha, Y. Anami, C.M. Yamazaki, W. Xiong, C.M. Haase, S.D. Olson, J. Lee, N. T. Ueno, N. Zhang, Z. An, K. Tsuchikama, An enzymatically cleavable tripeptide linker for maximizing the therapeutic index of antibody-drug conjugates, Mol Cancer Ther 21 (2022) 1449–1461, https://doi.org/10.1158/1535-7163.MCT-22-0362.
[39] J.G. Darker, S.J. Brough, J. Heath, D. Smart, Discovery of potent and selective peptide agonists at the GRP-preferring bombesin receptor (BB2), J. Pept. Sci. 7 (2001) 598–605, https://doi.org/10.1002/psc.359.
[40] A.A. Begum, P.M. Moyle, I. Toth, Investigation of bombesin peptide as a targeting ligand for the gastrin releasing peptide (GRP) receptor, Bioorg. Med. Chem. 24 (2016) 5834–5841, https://doi.org/10.1016/j.bmc.2016.09.039.
[41] A.A. Begum, Y. Wan, I. Toth, P.M. Moyle, Bombesin/oligoarginine fusion peptides for gastrin releasing peptide receptor (GRPR) targeted gene delivery, Bioorg. Med. Chem. 26 (2018) 516–526, https://doi.org/10.1016/j.bmc.2017.12.013.
[42] T. Günther, M. Konrad, L. Stopper, J.P. Kunert, S. Fischer, R. Beck, A. Casini, H. J. Wester, Optimization of the pharmacokinetic profile of [99mTc]Tc-N4-bombesin derivatives by modification of the pharmacophoric gln-trp sequence, Pharmaceuticals 15 (2022), https://doi.org/10.3390/ph15091133.
[43] S.D. Fontaine, R. Reid, L. Robinson, G.W. Ashley, D.V. Santi, Long-term stabilization of maleimide–thiol conjugates, Bioconjug Chem 26 (2015) 145–152, https://doi.org/10.1021/bc5005262.
[44] R.P. Lyon, J.R. Setter, T.D. Bovee, S.O. Doronina, J.H. Hunter, M.E. Anderson, C. L. Balasubramanian, S.M. Duniho, C.I. Leiske, F. Li, P.D. Senter, Self-hydrolyzing maleimides improve the stability and pharmacological properties of antibody-drug conjugates, Nat. Biotechnol. 32 (2014) 1059–1062, https://doi.org/10.1038/nbt.2968.

[45] K. Zheng, Y. Chen, J. Wang, L. Zheng, M. Hutchinson, J. Persson, J. Ji, Characterization of ring-opening reaction of succinimide linkers in ADCs, J Pharm Sci 108 (2019) 133–141, https://doi.org/10.1016/j.xphs.2018.10.063.
[46] R. Cescato, T. Maina, B. Nock, A. Nikolopoulou, D. Charalambidis, V. Piccand, J. C. Reubi, Bombesin receptor antagonists may be preferable to agonists for tumor targeting, J. Nucl. Med. 49 (2008) 318–326, https://doi.org/10.2967/jnumed.107.045054.
[47] J. Lau, E. Rousseau, Z. Zhang, C.F. Uribe, H.T. Kuo, J. Zeisler, C. Zhang, D. Kwon, K.S. Lin, F. Bénard, Positron emission tomography imaging of the gastrin-releasing peptide receptor with a novel bombesin analogue, ACS Omega 4 (2019) 1470–1478, https://doi.org/10.1021/acsomega.8b03293.
[48] B.A. Nock, A. Kaloudi, E. Lymperis, A. Giarika, H.R. Kulkarni, I. Klette, A. Singh, E. P. Krenning, M. De Jong, T. Maina, R.P. Baum, Theranostic perspectives in prostate cancer with the gastrin-releasing peptide receptor antagonist NeoBOMB1: preclinical and first clinical results, J. Nucl. Med. 58 (2017) 75–80, https://doi.org/10.2967/jnumed.116.178889.
[49] K. Abiraj, R. Mansi, M.L. Tamma, M. Fani, F. Forrer, G. Nicolas, R. Cescato, J. C. Reubi, H.R. Maecke, Bombesin antagonist-based radioligands for translational nuclear imaging of gastrin-releasing peptide receptor-positive tumors, J. Nucl. Med. 52 (2011) 1970–1978, https://doi.org/10.2967/jnumed.111.094375.
[50] G. Halmos, J.L. Wittliff, A. V Schally, Characterization of bombesin/gastrin-releasing peptide receptors in human breast cancer and their relationship to steroid receptor expression, Cancer Res. 55 (1995) 280–287.
[51] A. Plonowski, A. Nagy, A. V Schally, B. Sun, K. Groot, G. Halmos, In vivo inhibition of PC-3 human androgen-independent prostate cancer by a targeted cytotoxic bombesin analogue, AN-215, Int. J. Cancer 88 (2000) 652–657, https://doi.org/10.1002/1097-0215(20001115)88:4<652::aid-ijc21>3.0.co;2-657.